Journal of Ceramic Processing Research. Vol. 19, No. 1, pp. 75~79 (2018)

J O U R N A L O F
Ceramic
Processing Research

Weibull statistical analysis for vickers hardness of Al_2O_3/SiC composite according to the SiC concentration

Kwang-Ho Lee[a] and Ki-Woo Nam[b,*]

[a]*Daewoo Shipbuilding & Marine Engineering Co., Ltd., Gyeongsangnam-do 53302, Korea*
[b]*Department of Materials Science and Engineering, Pukyong National University, Busan 48547, Korea*

Hardness is a characteristic value that indicates resistance to partial deformation or abrasion of the material surface. It is easy to measure, and data can quickly be obtained. It also shows correlation with mechanical properties, such as tensile strength. Al_2O_3/SiC composite with three concentrations of silicon carbide was sintered, and heat-treated at three different temperatures. The Vickers hardness of the as-received specimen and the heat-treatment specimen was analyzed by Weibull statistics, and its probability distribution characteristics were evaluated. Since an oxide layer was formed on the surface by the heat-treatment, the hardness of the specimen having high temperature heat-treatment was low. The shape parameter and the mean Vickers hardness decreased as the heat-treatment temperature increased, and the scale parameters showed smaller than those of the as-received specimen. The scale parameters of the 1,473 K specimen were larger than those of the as-received specimen, but those of the (1,573 and the 1,673) K specimens were smaller than those of the as-received specimen. The entire shape parameters, except for the 1,673 K specimen of AS15Y3, were smaller than those of the as-received specimen, and the dispersions were large.

Key words: Al_2O_3/SiC composite, SiC concentration, Weibull statistical analysis, Vickers hardness

Introduction

Aluminum oxide (Al_2O_3), commonly known as alumina, is extensively used as an engineering ceramic, due to its high performance at a cost-effective price. It could be argued that alumina is one of the most cost-effective of all ceramic materials, and as a result, is one of the most widely used. Its combination of high thermal conductivity and low thermal expansion imparts good thermal shock resistance. Characteristics of alumina include: electrical insulation, high thermal conductivity, high strength and stiffness, availability in a range of purities, and excellent resistance to strong acids and alkalis at elevated temperatures. However, since ceramics are brittle, and have low toughness compared to metal materials, the reliability is low, and the use of critical equipment is limited. In order to overcome these weaknesses, the alumina ceramics require improved strength and heat resistance limit, large induced self-cracking ability, and overcoming of the low fracture toughness problem.

Monolithic Al_2O_3 and Al_2O_3/SiC composites have very interesting crack-healing ability [1-8]. SiC has crack-healing ability [9]. The crack-healing behavior of Al_2O_3/SiC composites is assumed to be sufficient by adding SiC [10, 11]. Applying the higher crack-healing ability of ceramics to structural components for engineering use could result in great benefits, such as increased reliability of the structural ceramic components, and reduced inspection, machining and polishing costs for the components. Niihara [12] has proposed a new concept: the so-called 'nanocomposite ceramics'. Some nanocomposite Al_2O_3/SiC exhibits excellent strength and heat resistance limit. However, the fracture toughness is low, and thus the Al_2O_3/SiC is very sensitive to flaws, such as cracks and pores.

The authors developed a new Al_2O_3/SiC [7, 8]. This has 15 wt.% SiC powder added to induce a large self-crack-healing ability, and (1-5) wt.% Y_2O_3 powder to prevent the grain growth of Al_2O_3 during sintering. The bending strength was the highest at 3 wt.% of yttria [7]. The crack healing properties and wear characteristics of sialon [13, 14], Si_3N_4 [15-18], SiC [10, 19], SiC_f/SiC [20], and ZrO_2/SiC [21, 22] were also evaluated. In particular, the strength distribution of the ceramic is not a definite value, but a stochastic quantity that shows variability [23]. The mechanical properties of materials are usefully used as basic data for reliability design, rationalization of design, and quality control of machines and structures. The authors statistically evaluated the ceramic properties under various conditions [24-26].

In this study, Al_2O_3/SiC was sintered by adding 3 wt.% of yttria, and changing the silicon carbide, which gives crack healing ability, to (10, 15, and 20) wt.%. As the properties of Al_2O_3/SiC Vickers hardness

*Corresponding author:
Tel : +82-51-629-6358
Fax: +82-51-629-6353
E-mail: namkw@pknu.ac.kr

were statistically variable, the statistical properties and probability distribution characteristics of Al_2O_3/SiC Vickers hardness were investigated.

Materials and Test Methods

Commercially available Al_2O_3 (AA-04, Sumitomo Chemical Co. Ltd., Japan), SiC (Ultrafine grade, Ibiden Co., Japan), and Y_2O_3 (Nippon Yttrium Co., Japan) were used as the starting materials. The mean particle size of the Al_2O_3 was 0.5 mm, while those of the SiC and Y_2O_3 powders were 0.27 mm. To evaluate the crack healing properties, (10, 15 and 20) wt.% SiC were added, respectively. Y_2O_3 was added in the amount of 3 wt.%. Hereinafter, each specimen shall be called AS10Y3, AS15Y3, and AS20Y3. The mixtures were milled in isopropanol for 24 h using Al_2O_3 ball (5 mm diameter). The mixtures were placed in a 363 K furnace to extract solvent, and to make a dry powder mixture. The dry powder was then passed through a 106 mm sieve. The mixtures were subsequently hot-pressed in N_2 gas for one h via hot-pressing, conducted under 35 MPa at 1,873 K. Table 1 shows each composition, while Fig. 1 shows a sintering flow chart.

The hot-pressed materials were machined to produce bar specimens (3 mm × 4 mm × 10 mm) that were polished. The condition of crack healing had a large effect on the fracture strength. Therefore, the micro-defects of the polished specimens were heat-treated at (1,473, 1,573, and 1,673) K for 1 h in air. The hardness of the heat-treated specimen was measured using a Vickers hardness tester (HV-114, Mitutoyo). The as-received specimen and the heat-treated specimen were measured for 10 s from the indentation loads of 19.6 N. Weibull statistical analysis was used, with hardness data of 20 measured on each specimen.

Table 1. Batch composition of Al_2O_3/SiC composite ceramics.

Powder	Al_2O_3 (wt.%)	SiC (wt.%)	Y_2O_3 (wt.%)
AS10Y3	87	10	3
AS15Y3	82	15	3
AS20Y3	77	20	3

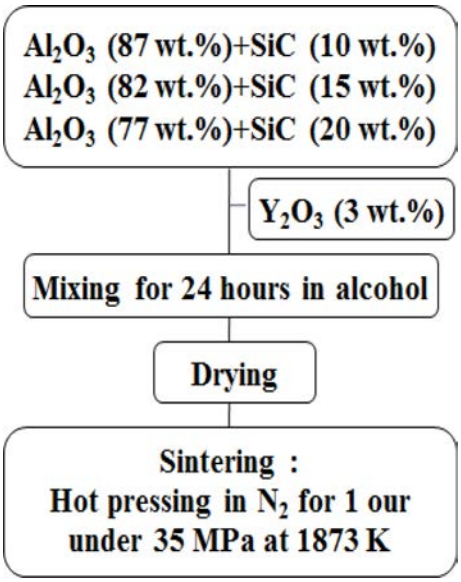

Fig. 1. Flow chart of sintering.

Test Results and Discussion

Fig. 2-4 show the Vickers hardness for the as-received specimen and the heat-treated specimen.

Fig. 2 shows the AS10Y3 specimen. The Vickers hardness of the as-received specimen shows a dispersion in the range (1,400-1,600) Hv, while that of the 1,473 K specimen shows a dispersion in the range (1,700-2,000) Hv higher than that of the as-received specimen. That of the 1,573 K specimen is smaller than that of the 1,473 K specimen, but shows a dispersion in the range (1,600-1,800) Hv, which is larger than that of the as-received specimen. That of the 1,673 K specimen shows the smallest dispersion in the range (900-1,300) Hv.

Fig. 3 shows the AS15Y3 specimen. The Vickers

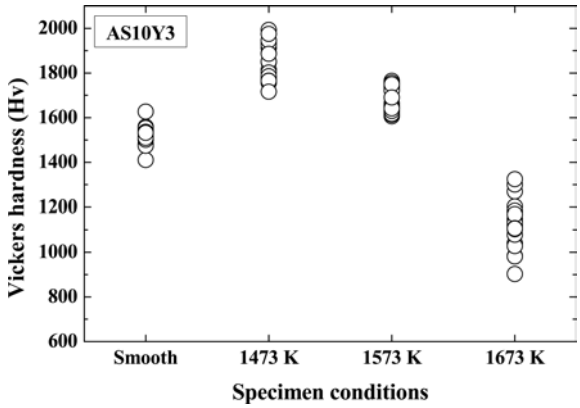

Fig. 2. Distribution of Vickers hardness according to specimen conditions in AS10Y3.

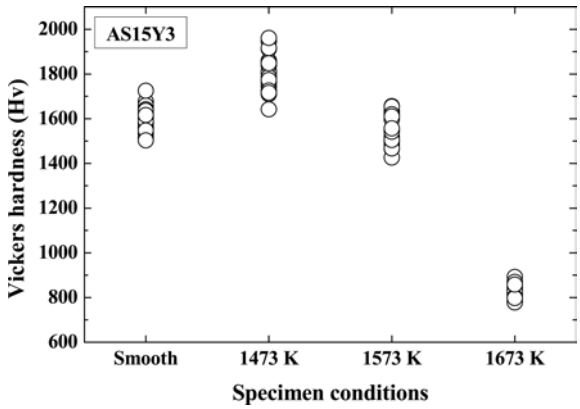

Fig. 3. Distribution of Vickers hardness according to specimen conditions in AS15Y3.

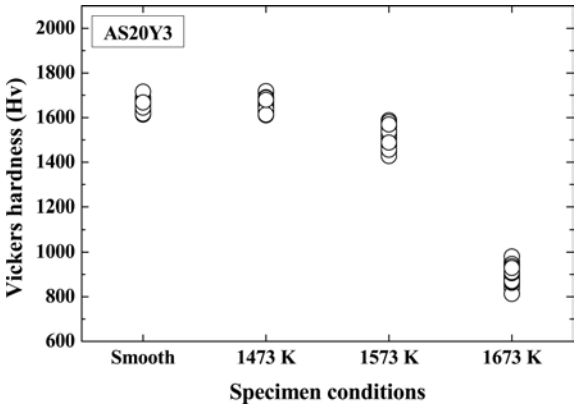

Fig. 4. Distribution of Vickers hardness according to specimen conditions in AS20Y3.

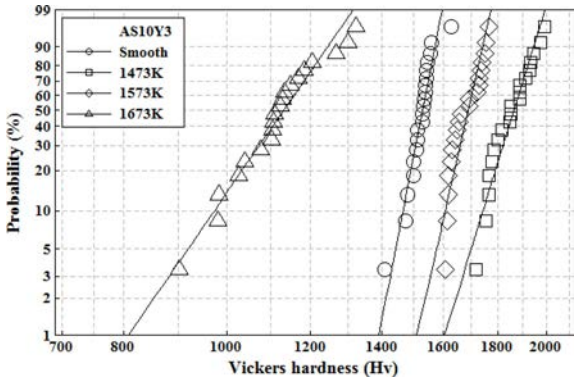

Fig. 5. Weibull plot of Vickers hardness from AS10Y3.

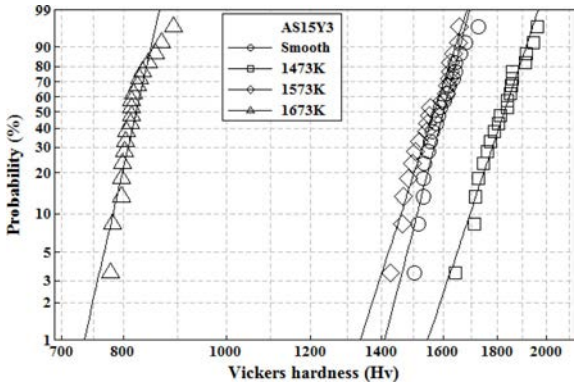

Fig. 6. Weibull plot of Vickers hardness from AS15Y3.

hardness of the as-received specimen shows a dispersion in the range (1,500-1,750) Hv, while that of the 1,473 K specimen shows a dispersion in the range (1,650-1,950) Hv, which is larger than that of the as-received specimen. That of the 1,573 K specimen shows a dispersion in the range (1,400-1,650) Hv, which is smaller than that of the 1,473 K specimen and the as-received specimen, and that of the 1,673 K specimen shows the smallest dispersion, in the range (780-900) Hv.

Fig. 4 shows the AS20Y3 specimen. The Vickers hardness of the as-received specimen shows a dispersion in the range (1,600-1,720) Hv, while that of the 1,473 K specimen shows a similar range of dispersion to that of the as-received specimen. That of the 1573 K specimen shows a low dispersion in the range (1,450-1,600) Hv, similar to the AS10Y3 and AS15Y3 specimens, and that of the 1673 K specimen also shows the smallest dispersion, in the range (800-1,000) Hv.

For the hardness evaluation of the ceramics, as a brittle material, a probabilistic evaluation considering the variation distribution is important, in order to increase the accuracy of the assessment. In addition, it can be seen that the Vickers hardness is not a determined value, but changes statistically. Accordingly, considering the ease of analysis and the weakest link assumptions, the Weibull statistical analysis needs to be applied as a two-parameter Weibull distribution, as shown below:

$$F(x) = 1 - exp\left[-\left(\frac{x}{\beta}\right)^{\alpha}\right]$$

Here, α is the shape parameter, which refers to the variability of the probability parameter, and β is the scale parameter indicating the characteristic lifetime, which is the failure probability of 63.2%.

Fig. 5-7 show the Vickers hardness of the AS10Y3, AS15Y3, and AS20Y3 specimen, respectively, according to the Weibull probability. Since hardness is expressed as a straight line, it can be seen as applicable to the Weibull probability distribution.

Fig. 5 shows the hardness distributions of the (1,473 and 1,573) K specimens, which reveal higher probability distributions than those of the as-received specimens, but that of the 1,673 K specimens show lower probability distributions than that of the as-received specimens.

Fig. 6 shows that the hardness distribution of the 1,473 K specimen reveal a higher probability distribution than that of the as-received specimen, but the 1,573 K specimen shows a probability distribution similar to that of the as-received specimen. However, the 1,673 K specimen shows a much lower distribution than that of the other specimens.

Fig. 7 shows that the hardness distributions of the 1,473 K specimen and the as-received specimen reveal similar probability distribution values, but the (1,573 and 1,673) K specimens show lower probability distribution values than that of the as-received specimen. In particular, the hardness distribution of the 1,673 K specimen is much lower than that of the other specimens.

In the author's paper, the 1,573 K crack-healing specimen showed the highest bending strength, but the hardness distribution was different. The bending strength is divided by the fracture cross-sectional area, but the hardness is the value measured at the surface. That is, it is considered that since the oxide layer is formed on the surface by the heat-treatment [27-29], the hardness of the test piece having a high heat-treatment temperature

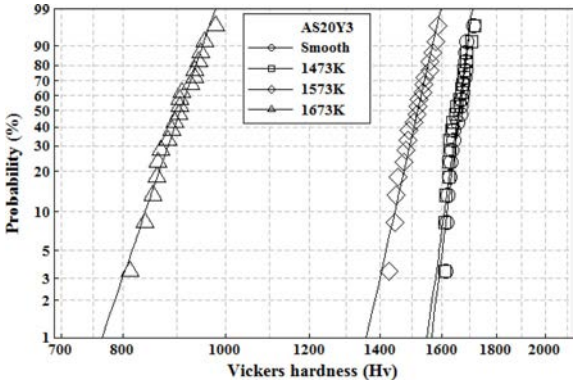

Fig. 7. Weibull plot of Vickers hardness from AS20Y3.

Table 2. The estimated Weibull parameters from Vickers hardness in AS10Y3.

Parameter / specimen	Shape parameter	Scale parameter	Std/Mean/COV
Smooth	44.8	1542	41.87/1524/0.027
1473K	28.2	1889	79.61/1854/0.043
1573K	38.2	1704	55.35/1681/0.033
1673K	12.6	1166	105.9/1121/0.095

Table 3. The estimated Weibull parameters from Vickers hardness in AS15Y3.

Parameter / Specimen	Shape parameter	Scale parameter	Std/Mean/COV
Smooth	33.4	1618	59.18/1593/0.037
1473K	25.6	1852	84.11/1815/0.046
1573K	26.5	1591	69.95/1560/0.045
1673K	37.6	832	28.50/820/0.035

Table 4. The estimated Weibull parameters from Vickers hardness in AS20Y3.

Parameter / Specimen	Shape parameter	Scale parameter	Std/Mean/COV
Smooth	69.4	1672.6	29.06/1660/0.018
1473K	62.5	1668.7	33.11/1655/0.020
1573K	38.0	1533.7	47.56/1513/0.031
1673K	24.9	920.4	42.59/901.4/0.047

is low. The larger the SiC concentration, the higher the tendency.

Tables 2-4 show the shape parameter and the scale parameters of the Weibull distribution function estimated from the Vickers hardness ofAS10Y3, AS15Y3, and AS20Y3 specimens, respectively. The table also shows the average, standard deviation (Std), and coefficient of variation (COV) according to mathematical statistics.

Fig. 8 is a graph of Tables (2-4). The shape parameter of the 1,473 K specimen is the largest, and those of the as-received specimen and the 1,573 K specimen are similar. However, the 1,673 K specimen shows a very small value. The scale parameter tends to be smaller than that of the as-received specimen.

The scale parameters of the three kinds of specimens were compared with each as-received specimen. In the AS10Y3 specimen, the (1,473 and 1,573) K specimens show (23 and 10) %, respectively. However, the 1,673 K specimen shows -24%. In the AS15Y3 specimen, the 1,473 K specimen shows 15%. However, the (1,573 and 1,673) K specimens show (-1.7 and -49) %, respectively. In the AS20Y3 specimen, the (1,473 1,573, and 1,673) K specimens show (-0.3, -8.3, and -45) %, respectively.

The shape parameters of the three kinds of specimens were compared with each as-received specimen. In the AS10Y3 specimen, the (1,473, 1,573, and 1,673) K specimens show (-37, -15, and -72) %, respectively. In the AS15Y3 specimen, the (1,473 and 1,573) K specimens show (-23 and -21) %, respectively, while the 1,673 K specimen shows 12.6%. In the AS20Y3 specimen, the (1473, 1,573, and 1,673) K specimens show (-10, -45, and -64) %, respectively.

In this way, the scale parameter of the 1,473 K specimen, which shows the characteristic life at the probability of 63.2%, was larger than those of the as-received specimen, but the (1,573 and 1,673) K specimens were smaller than those of the as-received specimen. On

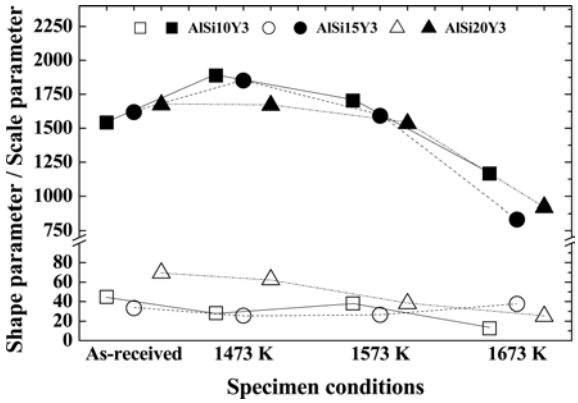

Fig. 8. Shape parameter and scale parameter from Weibull probability according to specimen conditions in AS10Y3, AS15Y3 and AS20Y3.

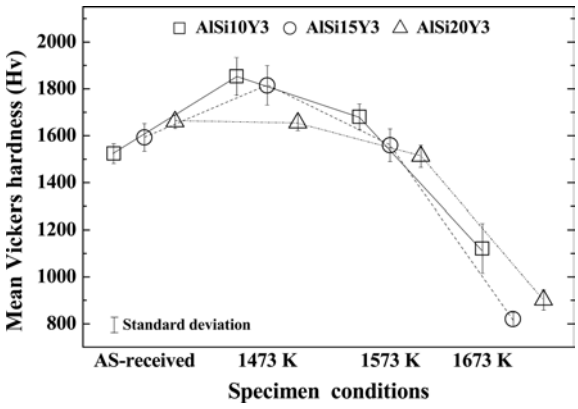

Fig. 9. Mean Vickers hardness according to specimen conditions in AS10Y3, AS15Y3 and AS20Y3.

the other hand, all of the shape parameters, except for the 1,673 K specimen of AS15Y3, were smaller than those of the as-received specimen, and the dispersion was large.

Fig. 9 shows the mean hardness in Tables 2-4, and also shows the standard deviation. The mean Vickers hardness of the 1,473 K specimen by the indentation load of 19.6 N is the largest, and those of the as-received specimen and the 1,573 K specimen are similar, but the 1,673 K specimen exhibits very small values. This is similar to the scale parameter.

The Vickers hardness of the three specimens was compared with that of the as-received specimen. In AS10Y3 specimen, the (1,473 and 1,573) K specimens show (22 and 10) %, respectively, while the 1,673 K specimen shows -26%. In the AS15Y3 specimen, the 1,473 K specimen shows 14%, while the (1,573 and 1,673) K specimens show (-1.3 and -49) %, respectively. In the AS20Y3 specimen, the (1,473, 1,573, and 1,673) K specimens show (-0.3, -9, and -44) %, respectively.

Therefore, as the heat-treatment temperature increases, the shape parameter and the mean Vickers hardness decrease, and the scale parameters are smaller than that of the as-received specimen. This is considered to be related to the oxide layer of the surface, as mentioned above.

Conclusions

In this study, Al_2O_3/SiC composite was sintered by adding the SiC concentration of (10, 15, and 20) wt.%, and heat-treated at the three different temperatures. The Vickers hardness of the as-received specimen and the heat-treatment specimen was analyzed by Weibull statistical analysis, and its probability distribution characteristics were investigated. The Vickers hardness of the as-received specimen and the heat-treatment specimen are not a determined value, but varied statistically. Since the oxide layer is formed on the surface by the heat-treatment, the hardness of the specimen having high heat-treatment temperature showed low. The larger the SiC concentration, the higher the tendency. As the heat-treatment temperature increases, the shape parameter and the mean Vickers hardness decrease, and the scale parameters show smaller than that of the as-received specimen. The scale parameters of the 1,473 K specimen, which show the characteristic life at the probability of 63.2%, are larger than those of the as-received specimen, but those of the (1,573 and 1,673) K specimens are smaller than those of the as-received specimen. The entire shape parameters, except for the 1,673 K specimen of AS15Y3, are smaller than those of the as-received specimen, and the dispersions are large.

References

1. F.F. Lange, and K.C. Radford, J. Am. Ceram. Soc. 53 (1970) 420-421.
2. T.K. Gupta, J. Am. Ceram. Soc. 59 (1976) 259-262.
3. J. Zhao, L.C. Stearns, M.P. Harmer, H.M. Chan, and G.A. Miller, J. Am. Ceram. Soc. 76 (1993) 503-510.
4. A.M. Thompson, H.M. Chan, M.P. Harmer, and R.F. Cook, J. Am. Ceram. Soc. 78 (1995) 567-571.
5. J.E. Moffatt, W.J. Plumbridge, and R. Hermann, Br. Ceram. Trans. 95 (1996) 23-29.
6. I.A. Chou, H.M. Chan, and M.P. Harmer, J. Am. Ceram. Soc. 81 (1998) 1203-1208.
7. K.W. Nam, H.S. Kim, C.S. Son, S.K. Kim, and S.H. Ahn, Transactions of the KSME(A), 31 (2007) 1108-1114.
8. H.S. Kim, M.K. Kim, S.B. Kang, S.H. Ahn, and K.W. Nam, Mater. Sci. Eng. A, 483-484 (2008) 672-675.
9. F.F. Lange, and K.C. Radford, J. Am. Ceram. Soc. 53 (1970) 290.
10. S.K. Lee, W. Ishida, S.Y. Lee, K.W. Nam, and K. Ando, J. Euro. Ceram. Soc. 25 (2005), 569-576.
11. K.W. Nam, and J.S. Kim, Mater. Sci. Eng. A, 527 (2010) 3236-3239.
12. K. Niihara, J. Am. Ceram. Soc. 99 (1991) 974-982.
13. S.W. Park, S.J. Moon, S.H. Ahn, J.S. Kim, and K.W. Nam, J. Korean Soc. Power Syst. Eng. 12 (2008) 50-54.
14. K.W. Nam, S.H. Park, S.W. Park, and S.J. Moon, Transactions of the KSME(A), 33 (2009) 957-962.
15. Y.Z. Zhang, L. Edwards and W.J. Plumbridge, J. Am. Ceram. Soc. 81 (1998), pp. 1861-1868.
16. K. Ando, T. Ikeda, S. Sato, F. Yao and Y. Kobayashi, Fatigue Fract. Engng. Mater. Struct. 21 (1998) 119-122.
17. K. Houjou, K. Ando, S.P. Liu and S. Sato, J. Euro. Ceram. Soc. 24 (2004) 2329-2338.
18. K.W. Nam, and J.S. Kim, J. Ceram. Process. Res. 11 (2010) 20-24.
19. K.W. Nam, J. Ceram. Process. Res. 13 (2012) 571~574.
20. K. Houjou, K. Ando and K. Takahashi, J. Soc. Mater. Sci. (Jap.) 58 (2009) 510-515.
21. K. Houjou and K. Takahashi, Inter. J. Struct. Intergrity 3 (2012) 41-52.
22. C,K, Moon, and K.W. Nam, J. Korean Soc. Nondestruc. Test. 34 (2014) 23-30.
23. S.J. Kim, D.S. Kim, and K.W. Nam, Transactions of the KSME(A), 39 (2015) 955~962.
24. S.H. Ahn, and K.W. Nam, J. Ceram. Process. Res. 17 (2016) 365-368.
25. S.C. Jeong, S.H. Ahn, and K.W. Nam, J. Ceram. Process. Res. 17 (2016) 1088-1094.
26. S.H. Ahn, C.Y. Kang, and K.W. Nam, J. Ceram. Process. Res. 18 (2017) 425-430.
27. M. Nakatani, K. Ando, and K. Houjou, J. Euro. Ceram. Soc. 28 (2008) 1251-1257
28. K. Takahashi, H. Murase, S.Yoshida, K. Houjou, K. Ando, and S. Saito, J. Euro. Ceram. Soc. 25 (2005) 1953–1959.
29. K. Houjou, K. Ando, M.C. Chu, S.P. Liu, and S. Sato, J. Euro. Ceram. Soc. 25 (2005) 559-567.